International Journal of Mechanical, Industrial and Aerospace Sciences
ISSN: 2517-9950
Vol:11, No:2, 2017

Coupled Spacecraft Orbital and Attitude Modeling and Simulation in Multi-Complex Modes

Amr Abdel Azim Ali, G. A. Elsheikh, Moutaz Hegazy

***Abstract*—**This paper presents verification of a modeling and simulation for a Spacecraft (SC) attitude and orbit control system. Detailed formulation of coupled SC orbital and attitude equations of motion is performed in order to achieve accepted accuracy to meet the requirements of multitargets tracking and orbit correction complex modes. Correction of the target parameter based on the estimated state vector during shooting time to enhance pointing accuracy is considered. Time-optimal nonlinear feedback control technique was used in order to take full advantage of the maximum torques that the controller can deliver. This simulation provides options for visualizing SC trajectory and attitude in a 3D environment by including an interface with V-Realm Builder and VR Sink in Simulink/MATLAB. Verification data confirms the simulation results, ensuring that the model and the proposed control law can be used successfully for large and fast tracking and is robust enough to keep the pointing accuracy within the desired limits with considerable uncertainty in inertia and control torque.

***Keywords*—**Attitude and orbit control, time-optimal nonlinear feedback control, modeling and simulation, pointing accuracy, maximum torques.

I. Introduction

MODELING and simulation are essential steps for SC Attitude and Orbit Control (AOC) iterative designing process, off nominal situation analyses, new techniques/future missions testing or control ground stations (CGS) operational control actions creation. All SCs obey the basic physical laws of celestial mechanics. With these basic laws it is possible to precalculate the position of a body in its orbit. Mathematics of SC orbits start with the basics of Newton's laws and the original Keplerian orbit model. Using classic orbital elements, the required calculations needed to describe the orbit can be derived. The fundamental laws of physics upon which the theory of orbital mechanics is based are Newton's law of universal gravitation and Newton's law of motion [1], [2]. The fundamental properties of orbits are summarized in Kepler's three laws of planetary motion [3]. The six Keplerian elements are different integration constants which specify completely the properties of an elliptical orbit. These elements include semi-major axis a, Eccentricity e which describe the orbit shape, Inclination i, Right ascension of ascending node and Argument of Perigee ω which describe the orbit orientation and Epoch t_0 that describes the time of Perigee. When the gravitational force, as assumed by Newton's law, is acting on the SC the first five parameters will be constant and the orbit is an ideal Keplerian orbit. Only the true anomaly of the SC changes its value due to the undisturbed movement in the orbit. If disturbance forces are present, the motion becomes an osculating orbit. Due to the disturbance forces the shape and the orientation of the orbit will change and the Keplerian elements become time-variant [3]. NASA and the US Space Command derived the Simplified General Perturbation models (SGPs) for precise orbit calculations [4], [5]. The work in this paper aims to build a simulator from one side to maintain the freedom to reconfigure itself according to different SC, missions, guidance strategies, control algorithms, complex/orientation modes or hardware in used, and from another side, can use the required module from available predetermined modules, e.g. MATLAB/Simulink modules or result data of available analytical propagators, which are documented for general use, e.g. SGPs. Orbit propagation, was created by the integration of equations of motion or by imports of the SC state vector using the Two Line Element (TLE) set and (SGP4) Version 4. The simulation results represented in Earth Centered Earth Fixed (ECEF) and Earth Centered Inertial (ECI) frames. The dominant disturbance torques effect on the SC in its working orbit was taken into consideration. The attitude control system specifications were selected based on the transient response and steady state requirements. Based on quaternion feedback control [6]. The feedback gains were selected to confirm the global stability conditions. The effect of the actuator saturation limit and maximum slew rate was discussed. For better sense, the attitude representations were converted from quaternion to Euler angles.

Amr Abdel Azim Ali is with Military Technical College, Egyptian Armed Forces, Cairo, Egypt (e-mail: amrabdelazimali@gmail.com).
Gamal Ahmed Elsheikh is with P.H.I., Giza, Egypt (e-mail: gaelsheikh@gmail.com).
Moutaz Hegazy is with Military Technical College, Egyptian Armed Forces, Cairo, Egypt (e-mail: moutaz27@yahoo.co.uk).

II. SC Combined Nonlinear Model

A. Coordinate Systems

In order to build a SC motion control system, the following right-handed coordinate systems are used:

- Body coordinates system (BCS): Principal inertia coordinate system centered in the SC mass center.

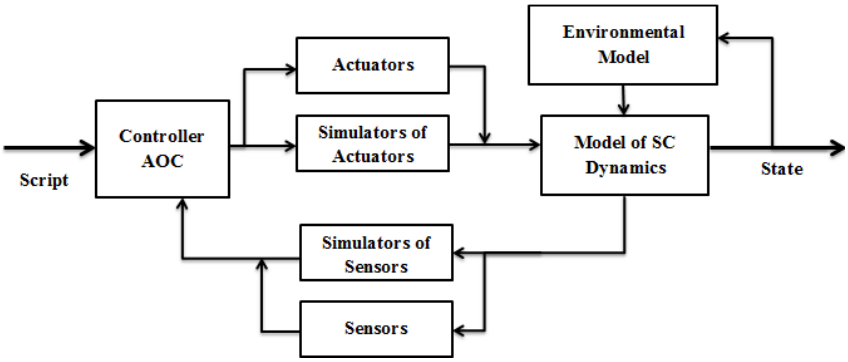

Fig. 1 Simulator block diagram

- Inertial coordinates system (ICS): Inertial equatorial coordinate system, related to mean equator and equilibrium in standard epoch of J2000 Center of coordinate system is situated in the center of the Earth. In this coordinate system, the coordinates of stars of onboard catalog are saved:
  - +X axis directed to the point of spring mean equilibrium,
  - +Z axis directed to the northern pole of the world.
- Earth Centered Earth Fixed (ECEF) coordinates system (Geographic/geodesic coordinates system (WGS84)) in which:
  - +X axis lies in the plane of geographic equator and is defined by the reference-meridian of international Earth rotation service,
  - +Z axis is directed to the reference-pole of international Earth rotation service and perpendicular to the plane of the geographic equator, and
  - +Y axis completes the right hand coordinate system and lies in plane of geographic equator.
- Orbital coordinates system (OCS): Coordinate system centered in the SC mass center:
  - +Y axis is directed along the radius-vector to the center of the Earth, and
  - +X coincides with the vector of orbital angular rate.
- Target coordinates system (OCS-N): Coordinate system centered in the SC mass center:
  - +Y axis is directed to the object of shooting, and projection of axis
  - -Z is the acute angle with the direction of the vector of orbital angular rater (angle between axis -Z and orbit plane is equal to the required additional turn angle in yaw to prevent a smeared picture).
- Inertial Coordinates System of Strap-down Inertial Navigation System (SINS ICS): Computational Coordinates System equivalent to gyro-stabilized platform.
- Device coordinates systems for orientation sensors (DCS OS): Correspond to the position of measuring axes of orientation sensors.

B. Orbit Propagation via Integration of Equations of Motion

Orbit propagation is carried out by the integration of the equation of motion from the initial state vectors x_0 and v_0 at time t_0 to the final state vectors x and v at time t_k using Runge-Kutta4 method with the step up to 20 sec for one revolution prediction and up to 100 sec for one day prediction. Prediction is carried out using geo-potential function, to describe the biggest source of error which is due to the fact that the Earth is not perfectly circular. The deformation can be described by using the zonal harmonic coefficients J_i for ith deformations order. The orbital equations of motion in ECEF (Greenwich) are described as [1]:

$$\begin{aligned}
\dot{x}_G &= v_{xG} \\
\dot{y}_G &= v_{yG} \\
\dot{z}_G &= v_{zG} \\
\dot{v}_{xG} &= -(\mu/r^3)x_G + (3/2)J_2\,(\mu a_e^2/r^5)\,x_G(1-5Z_G^2/r^2) \\
&\quad + \omega_z^2 x_G + 2\omega_z v_{yG} \\
\dot{v}_{yG} &= -(\mu/r^3)y_G + (3/2)J_2\,(\mu a_e^2/r^5)\,y_G(1-5Z_G^2/r^2) \\
&\quad + \omega_z^2 y_G - 2\omega_z v_{xG} \\
\dot{v}_{zG} &= -(\mu/r^3)z_G + (3/2)J_2\,(\mu a_e^2/r^5)\,z_G(3-5Z_G^2/r^2)
\end{aligned} \tag{1}$$

where $r = \sqrt{x_G^2 + y_G^2 + z_G^2}$, μ is the Earth's gravitational field constant, a_e is the equatorial radius of the Earth, ω_z is the Earth's rotation angular velocity, J_2 is the second zonal harmonic of geo-potential expansion into a series in the spherical functions, it is a dimensionless parameter quantifies the major effects of oblateness on orbits, it is not a universal constant. Each planet has its own values of oblateness and J_2. For Earth, oblateness is equal 0.003353 and J_2 is equal $1.08263x10^{-3}$. Prediction accuracy increases if all terms of the perturbations are included and the acceleration of the SC is calculated including dominant effects like the effects of the Earth, Moon, Sun gravity fields and lesser effects like tides, atmospheric drag, light pressure and relative disturbance acceleration. Orbit Propagation via this method generates an increasing error of nearly 3 km per orbit and increases of nearly 8 km per day.

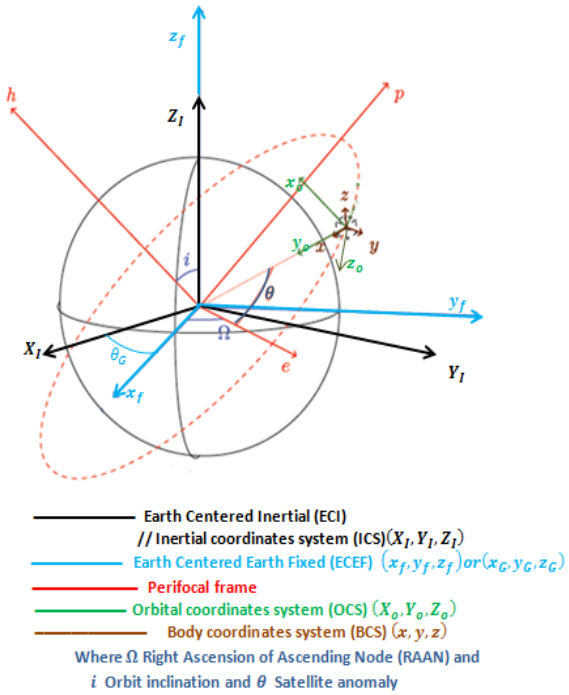

Fig. 2 Reference coordinate systems

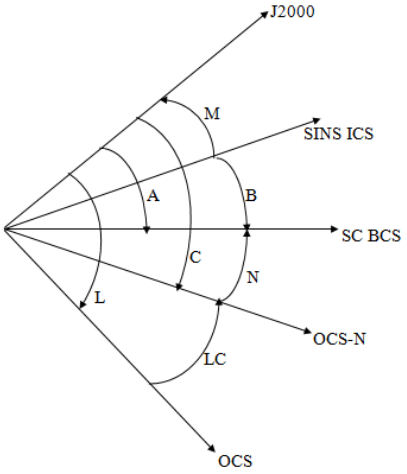

Fig. 3 Quaternions representation

TABLE I
QUATERNIONS REPRESENTATION

Quaternion	Description
A	Quaternion of transition from ICS to BCS
B	Quaternion of transition from strap-down inertial navigation system SINS ICS to BCS.
C	Target quaternion, Quaternion of transition from ICS to target.
L	Calculated orbital quaternion of transition from ICS to OCS, calculated by navigation state vector.
M	Quaternion of transition from SINS ICS to ICS, mismatch quaternion between ICS & SINS ICS
N	Control quaternion; Mismatch quaternion between desired (calculated) orientation and current BCS orientation; calculated according to mode.
LC	Target quaternion, Quaternion of transition from OCS to target.

C. The NORAD Orbit Propagation

For precise orbit calculations, other forces beyond the Earth's gravitation which cause perturbations must be taken into account. In order to avoid such errors in the propagation of SCs, the North American Aerospace Defense (NORAD) command maintain general information about the perturbation on all space objects and a SGP developed by Hilton and Kuhlman [5], [4]. The Russians developed a series of analytical propagators, each tuned for a specific SC regime. The narrower focus permits additional attention to detail, and higher resulting accuracy. But none of these analytical routines can eventually be documented for general use in the same manner as SGPs.

SGPs

Given the Keplerian elements for a single point in time, the estimation of the future position becomes straight forward [2]. Reference [2] describes the SGP model and how the Kepler's calculations are contained in this model (see also [5]). The SGP4 model was an extension of the SGP model in order to get a more precise estimation, the atmospheric drag could be estimated by using the ballistic coefficient B* and a term for the perturbations due to solar radiation are included (for details see [7]). Perturbations can be classified according to their effects on the orbital elements as [7]:

Periodic perturbations cause a sinusoidal variation in orbital elements over time and consist of:

1) Short-term periodic perturbations have a period less than the orbit period.
2) Long-term periodic perturbations have a period greater than one orbit period.

Secular perturbations cause secular variation. Its long-term non-periodic variation does not depend on time. If it has a linear long-term trend, it is called secular drift. Secular variation in centuries may be part of a periodic variation in millions of years.

NORAD Two-Line Orbital Element Set (TLE)

A Two-Line Element (TLE) set is a format that is used to describe the position of a SC at a particular instant of time [8]. This format consists of two lines of 69 characters of data containing the mean orbital element; the first line contains various identification data sets and also the perturbation influences by the geopotential and the drag forces. The second line contains the Keplerian elements to describe the orbital plane. The only parameter which is missing is the semi-major axis (a), but this parameter can be determined by the mean motion [2]. The NORAD TLEs consists of mean orbital elements that average out these perturbation effects in a specific manner [4]. The right ascension and declination data of a SC is taken, via observing the SC through an optical or radio telescope, SLR technique or other advanced observing techniques, for a short time period. These data are then passed through computer software that generates mean orbital element sets and other necessary parameters needed for the TLEs.

D. Orbit Representation in Different Coordinate Systems

SC orbits are more easily interpreted as circular or elliptical when plotted in ECI. Figs. 4 and 5 are used to illustrate the

difference between the orbits representation in ECEF and ECI frames. The orbital period of the SC is 92 minutes; so the SC completes 15.6 revolutions per day. In Figs. 4 and 5, the SC orbits are plotted for the duration of one day, so there are 15.6 orbits in each figure. These orbital passes are generated by the SGP4 propagator that includes the perturbations effects on the SC like Earth's gravity and atmospheric drag. This perturbation effect is more clearly viewed in Fig. 5, where the plotted points do not overlap on each revolution. If the perturbation effects are excluded the points should coincide on each revolution.

Figs. 4 and 5 clarify that the SC orbits is more clearly seen as circular in the ECI system. The orbital state vectors in the ECI system generated by SGP4 can be converted to the ECEF system by using the following matrix equation [9]:

$$[\mathrm{r}_{\mathrm{ECEF}}] = [A_{GI}][\mathrm{r}_{\mathrm{ECI}}] \tag{2}$$

where $[A_{GI}]$ is the transformation matrix given as:

$$\mathrm{A}_{GI} = \begin{bmatrix} \cos\theta_G & \sin\theta_G & 0 \\ -\sin\theta_G & \cos\theta_G & 0 \\ 0 & 0 & 1 \end{bmatrix} \tag{3}$$

where θ_G, as illustrated in Fig. 2, denotes the Greenwich sidereal time at a specific epoch:

$$\theta_G = \theta_{G0} + \omega_e\, t \tag{4}$$

Here, θ_{G0} indicates the Greenwich sidereal time at 00:00:00 UT, ω_e denotes the inertial rotation rate of the Earth, and t is the time duration since 0 hours UT.

The SC travels in prograde orbit. It has an orbital inclination of less than 90° and travels in the same direction as the rotation of the Earth around its own axis i.e. from the West to East direction. Fig. 6 illustrates the prograde orbit having an inclination of 52°, which is less than 90°.

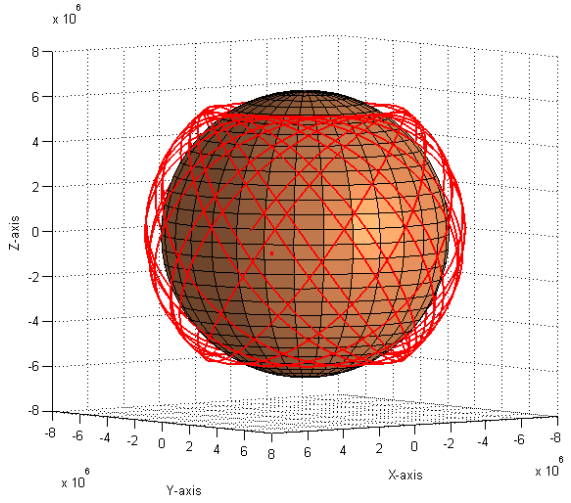

Fig. 4 SC orbit in the ECEF system

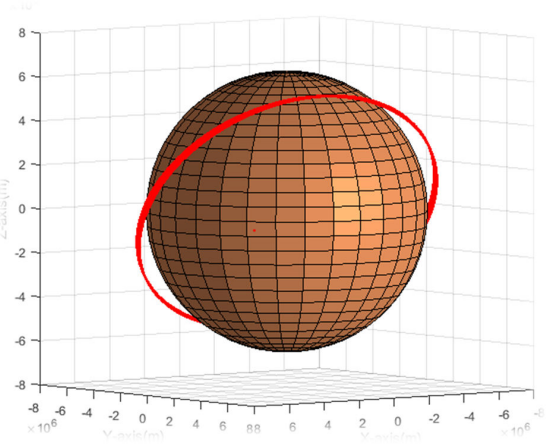

Fig. 5 SC orbit in the ECI system

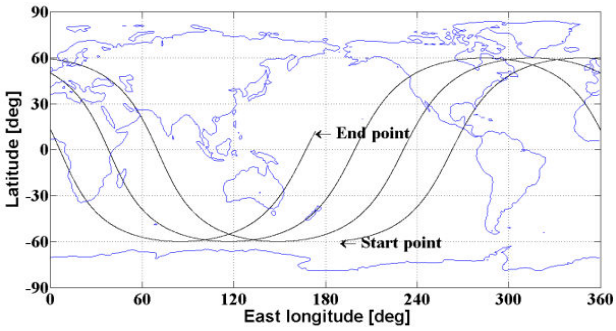

Fig. 6 Ground track of SC plotted in ECEF system

E. SC Attitude Dynamics and Kinematics

Recall from [10], the equations represent the basis for dynamic attitude modeling, and also form the so-called Euler equations of motion:

$$J\dot{\omega} = -\omega \times (J\omega) + M \tag{5}$$

$$\dot{\omega} = -J^{-1}(\Omega(\omega)J\omega) + M) \tag{6}$$

$$M = u + T_d \tag{7}$$

where J is the SC inertia matrix, M is the projection of the total applied moments on the principal central axes of the SC ellipsoid of inertia, u are the control torques, T_d is the disturbance torques, $\omega = \omega_{bI} = [\omega_1, \omega_2, \omega_3]^T$ is the SC absolute angular velocity (relative to the inertial reference frame) projected into the SC body coordinate system and measured by rate gyros, $\Omega(\omega)$ is a skew-symmetric matrix defined by:

$$\Omega(\omega) = [\omega^X] = \begin{bmatrix} 0 & -\omega_3 & \omega_2 \\ \omega_3 & 0 & -\omega_1 \\ -\omega_2 & \omega_1 & 0 \end{bmatrix} \tag{8}$$

Descriptions of SC attitude can be via various attitude parameters, e.g., quaternion or Euler angles parameters. Given Euler angles, a unique orientation is defined. Given the orientation, non-unique Euler angles can be determined due to

singularity. Euler angles representation is best for the analytical and attitude control design process. Quaternion representation is free from trigonometric components and singularity. It is computationally robust and ideal for digital control implementation. SC orientation via quaternion representation does not appear easily without professional reading or transformation to Euler angles. So, the existence of both representation (Euler angles and quaternion) at input/output of this simulation and the facility of transformation between them were considered. The kinematic equation is derived from observation of the attitude matrix change over time. For a kinematic consideration, attitude change is observed without the existence of the torque triggers. This change as a relation between the attitude and angular velocity of the body is given as:

$$\begin{aligned} \dot{q}_{vec} &= -(1/2)\Omega q_{vec} + (1/2)q_4\omega \\ \dot{q}_4 &= -(1/2)\omega^T q_{vec} \end{aligned} \tag{9}$$

The parameterization of the quaternions q is done as:

$$\begin{aligned} q_1 &= e_x \sin(\emptyset/2) \\ q_2 &= e_y \sin(\emptyset/2) \\ q_3 &= e_z \sin(\emptyset/2) \\ q_4 &= \cos(\emptyset/2) \end{aligned} \tag{10}$$

where e_x, e_y, e_z are the components of the Euler axis unit vector in the reference frame, and $\emptyset$ is the rotation angle around the Euler axis. Using (10), it is clear that the quaternion components satisfy the following constraint:

$$q_1^2 + q_2^2 + q_3^2 + q_4^2 = 1 \tag{11}$$

where $q = q_{scal} + q_{vec}$; $q_{scal} = q_4$ is the scalar part of the quaternion q, $q_{vec} = [q_1, q_2, q_3]^T$ is the vector part of the quaternion q.

Any vector in the reference frame (I) can be transformed to body coordinates by the transformation matrix A_{bI}, which can be written in terms of quaternion components as [9]:

$$A_{bI} = \begin{bmatrix} q_1^2 - q_2^2 - q_3^2 + q_4^2 & 2(q_1q_2 + q_3q_4) & 2(q_1q_3 - q_2q_4) \\ 2(q_1q_2 - q_3q_4) & -q_1^2 + q_2^2 - q_3^2 + q_4^2 & 2(q_2q_3 + q_1q_4) \\ 2(q_1q_3 + q_2q_4) & 2(q_2q_3 - q_1q_4) & -q_1^2 - q_2^2 + q_3^2 + q_4^2 \end{bmatrix} \tag{12}$$

Equation (12) can be represented by using various attitude parameters.

F. Disturbance Torques on a SC

In order to model the attitude dynamics of the SC, the disturbance torques $[\mathrm{T_d}]$ (internal and external) acting on the SC have to be considered. Internal disturbance torques are usually generated from movable mechanisms (generally not desired, e.g. fuel sloshing, structure mechanisms, solar panels). External disturbance torque is generated by the interaction of the space environment with the SC. The corresponding magnitude of the disturbance torques is mainly related to the orbit and attitude of the SC and its physical properties. There are number of external torques acting on a SC which disturbs the attitude motion. For a SC in the vicinity of the Earth, the major disturbance torques are Gravity-gradient torque (Mgrav), Magnetic torque (Mmag), Solar radiation pressure torque (Msol) and Aerodynamic torque (Maero). The rough ratio of the disturbance torques acting on a SC at 1000 km [11] is Mgrav : Mmag : Msol : Maero = 1000 : 250 : 2 : 0.5. So, the dominant disturbance torques in the case of an altitude of 700 km are Gravity-gradient torque and Magnetic torque.

G.Formulation of Coupled SC Orbital and Attitude Equations of Motion

The SC attitude motion is numerically simulated relative ICS under the influence of a gravity-gradient disturbance torque. The attitude kinematics is given by (9). It is clear from (9) that to solve the formula for determining the quaternion/Euler angles, the angular velocity [ω] is needed. This is governed by the attitude dynamics, as summarized in (6) and (7). The dominant part in the disturbance torques $\mathrm{T_d}$ is the gravity-gradient torque which is described by:

$$[\mathrm{T_g}] = 3\mu/\mathrm{r}^5 \; [\mathrm{r_b^X}]\,[\mathrm{J}][\mathrm{r_b}] \tag{13}$$

where μ is the Earth's gravitational constant, $[r_b]$ is the SC's orbital position vector expressed in BCS, $[r_b^X]$ a skew-symmetric matrix from $[r_b]$ and $r = \|[r_b]\|$ is the orbital radius. From (13), coupling between the SC orbital and attitude motion equations is clear and simulation of the SC orbit is required, as well as the attitude, in order to be able to compute $[T_g]$. The SC orbit can be simulated to sufficient accuracy by either SGP4 or NORAD-TLE set or the integration of the equations of motion including the weak effect perturbation sources. The SC orbital motion is described in ICS coordinates by [12]:

$$\begin{aligned} &[\ddot{r}] \\ &= -\mu[r]/r^3 \\ &+ (3\mu J_2 R_e^2/2r^5)\,[(5\,(([r^T][Z_G])^2/r^2) - 1)[r] \\ &- 2([r^T][Z_G])[Z_G]] \end{aligned} \tag{14}$$

where $[Z_G] = [0 \quad 0 \quad 1]$, $[r]$ is the SC's orbital position expressed in ICS, and R_e is the Earth's equatorial radius. Thus, the SC orbit is best simulated in the ICS as clarify from Fig. 4 and Fig. 5. Referring to (13), it is noted that in order to compute $[\mathrm{T_g}]$, converting the SC orbital position vector from ECI to BCS is required. The required transformation matrix (A_{bI}) is described by (12) and the SC orbital position vector in BCS can be determined from:

$$[r_b] = [A_{bI}][r] \tag{15}$$

Equations (6), (7), (9), and (12)-(15) are self-contained, and fully describe the coupled SC attitude and orbital motion.

Numerical simulation of SC motion involves numerical integration of the equations of motion. It is possible to write the equation of motion as a first-order differential equation of the form:

$$\dot{\mathrm{X}} = \mathrm{f}(\mathrm{X}, \mathrm{t});\; \mathrm{X}(\mathrm{t_0}) = \mathrm{X_0} \tag{16}$$

where the state vector X may contain the SC orbital position, velocity, attitude variables, angular velocity, and any other state variables (for example controller states) required to fully describe the SC motion. This is called a state-space representation of the system [12]. To numerically simulate the SC motion, we need to determine the time history of the state vector $X(t)$ for $t \geq t_0$ numerically. All numerical integration schemes are based upon a discretization of time with sample times t_k. The difference between subsequent sample times $h = t_k - t_{k-1}$ is called the time step and must be sufficiently small.

In order to write the equations as a first-time derivatives in the form of (16), the SC inertial velocity vector V is introduced:

$$[\dot{r}] = [\mathrm{v}] \tag{17}$$

Then, the second time-derivative of r becomes the first time-derivative of V, that is:

$$[\dot{V}] = [\ddot{\mathrm{r}}] \tag{18}$$

In addition, (14) becomes:

$$[\dot{V}] = -\mu[r]/r^3 + (3\mu J_2 R_e^2/2r^5)\left[(5\,(([r^T][Z_G])^2/r^2) - 1)[r] - 2([r^T][Z_G])[Z_G]\right] \tag{19}$$

By introducing the inertial velocity vector V, the second-order differential equation (14) can be replaced by the pair of first-order differential equations (17) and (19). The coupled SC attitude and orbital motion is therefore fully described by the first order differential equations (6), (9), (17), and (19), together with (12), (13), and (15). Since the quantities appearing with first time-derivatives are $(a1, a2, and\ a3)\ or\ q, \omega, r$, and V, these equations are in a suitable form to be programmed for use with a numerical ODE solver (such as those available in MATLAB). It is clear from (16) that the initial condition $X(0)$ must be specified. So, the initial Euler angles $(a1(0), a2(0), and\ a3(0))$ or initial quaternion $q(0)$, the initial angular velocity $\omega(0)$, the initial orbital $r(0)$, and the initial orbital velocity $V(0)$ are required.

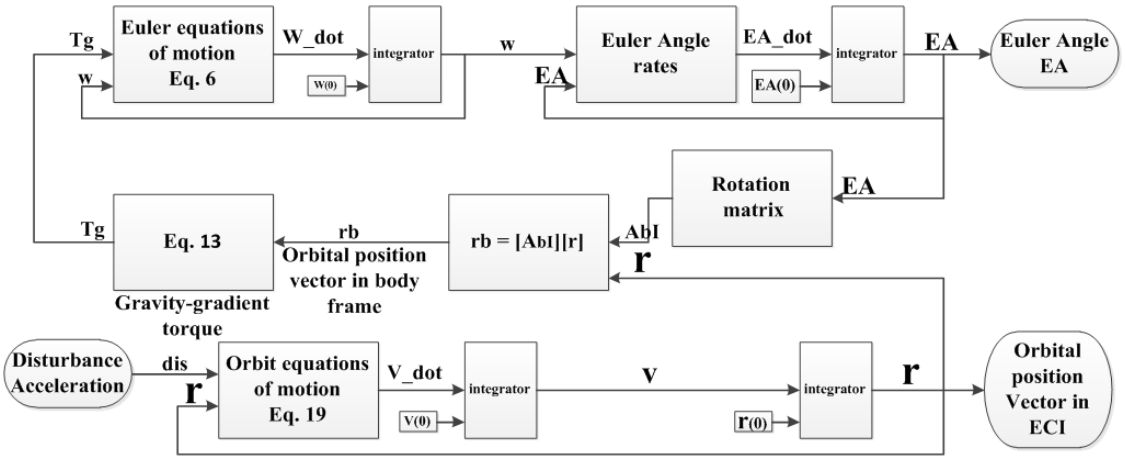

Fig. 7 Coupled SC Orbital and Attitude Equations of Motion

III. Time-Optimal Switching Control Logic with Linear Range

In practice, a direct implementation of an ideal time-optimal switching control logic results in a chattering problem [13] about the origin. This problem is returned back to time delays in the control system and various uncertainties in the moment of inertia **J** and actuator dynamics, where the maximum actuator torque **U** is not exactly known. To eliminate this effect, a conventional linear control solution will replace the bang-bang solution near the origin and any attitude maneuver divided to the following two parts:

A. Time-Optimal Control

A complete treatment of time-optimal reorientation in space, based on optimal control theory, can be found in [14]. Consider a rigid SC that is required to maneuver about an inertially fixed axis as fast as possible, but not exceeding the specified maximum slew rate about that eigenaxis. The following saturation control logic provides such a rest-to-rest eigenaxis rotation under slew rate constraint:

$$\tau = -J\{2k^{sat}_{Li}(e) + d\omega\} \tag{20}$$

where $\mathrm{e} = (\mathrm{e}_1, \mathrm{e}_2, \mathrm{e}_3)$ is the quaternion-error vector, for achieving rapid transient settlings for large attitude-error signals, the attitude error saturation limits $\mathrm{L_i}$ are determined corresponding to [15] as:

$$L_i = (d/2k)min\left\{\sqrt{4a_i|e_i|}, |\omega_i|_{max}\right\} \tag{21}$$

where $\mathrm{a_i} = \mathrm{U/J_{ii}}$ is the maximum control acceleration about the $\mathrm{i^{th}}$ control axis and $|\omega_\mathrm{i}|_\mathrm{max}$ is the specified as the maximum angular rate about each axis.

B. Linear Quaternion Feedback Control

The linear state feedback controller of the following form can be considered for the real-time implementation of eigenaxis rotations in the 2nd part of the maneuver (linear range):

$$u = -Kq_e - D\omega - \mu\Omega J\omega \tag{22}$$

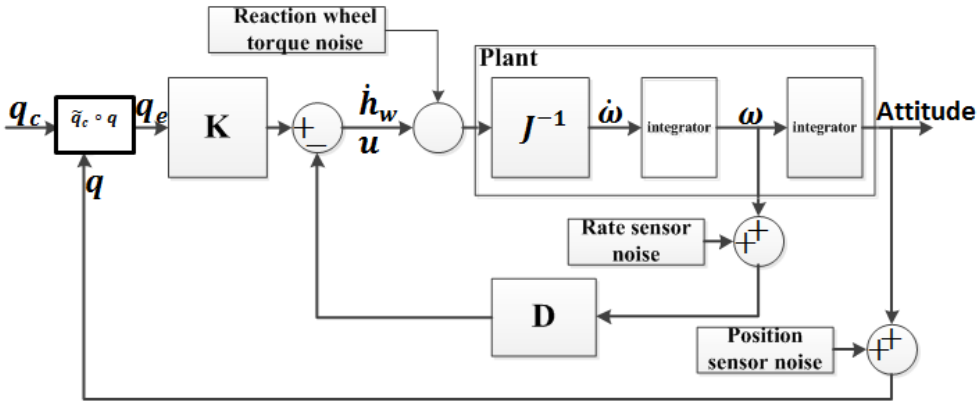

Fig. 8 Quaternion Feedback Control

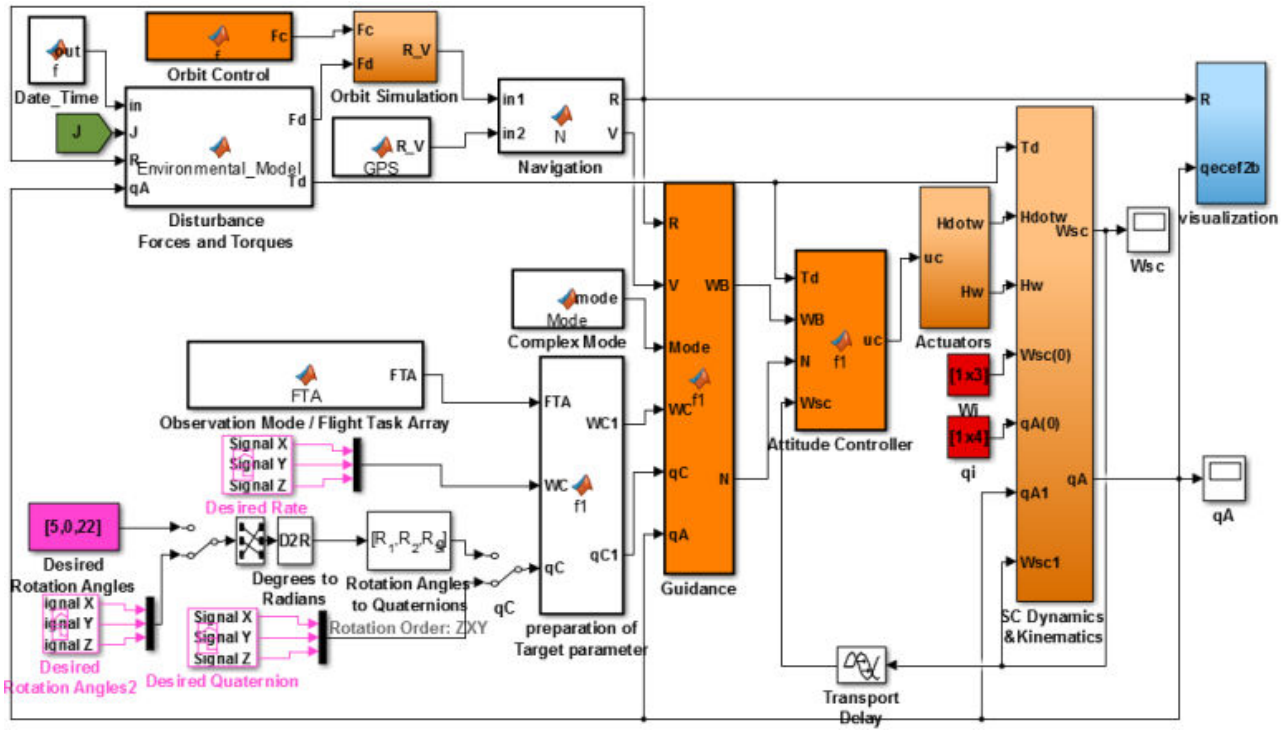

Fig. 9 Simulator main layer

The selected feedback controller for eigenaxis rotations consists of linear error-quaternion feedback, linear body-rate feedback, and a nonlinear body-rate feedback term that can be added to counteract the gyroscopic coupling torque. Considering $\mu = 1$ means that the control torque exactly counteracts the gyroscopic coupling torque, while $\mu = 0$ means that only quaternion feedback and linear rate feedback are used. This controller is a time invariant closed loop controller in which no reference trajectory is available for the mid-time until reaching the required final attitude, and the control at any time is calculated as a function of the current measured attitude and angular rate without any use of time dependent gains or functions. In general, $u = [u_1, u_2, u_3]^T$ is the control torque vector, where the torques $u_1, u_2,$ and u_3 are applied by the actuators about the x, y and z body fixed axes. The gains K and D are 3X3 controller gain matrices to be properly determined or designed. These gains are selected according to Wie [6] as: $D = dJ$ and $K = kJ$, where d and k are scalars for the eigenaxis rotation. $q_e = (q_{1e}, q_{2e}, q_{3e})^T$ is the attitude error quaternion vector which is a part of the attitude error quaternion $q_e = [q_{1e}, q_{2e}, q_{3e}, q_{4e}]$, which represents the attitude error between the current orientation and the desired one, and defined as [10]:

$$\begin{bmatrix} q_{1e} \\ q_{2e} \\ q_{3e} \\ q_{4e} \end{bmatrix} = \begin{bmatrix} q_{4c} & q_{3c} & -q_{2c} & -q_{1c} \\ -q_{3c} & q_{4c} & q_{1c} & -q_{2c} \\ q_{2c} & -q_{1c} & q_{4c} & -q_{3c} \\ q_{1c} & q_{2c} & q_{3c} & q_{4c} \end{bmatrix} \begin{bmatrix} q_1 \\ q_2 \\ q_3 \\ q_4 \end{bmatrix} \quad (23)$$

The equation is the result of successive quaternion rotations using the quaternion multiplication and inversion rules:

$$q_e = \tilde{q}_c \circ q \quad (24)$$

IV. Simulation

The simulator is built using Simulink toolbox/MATLAB version 8.5.0.197613 (R2015a). The simulator includes many subsystems. The main layer of the simulator is shown in Fig. 9 and consists of:

A. Environmental model module
B. Orbit simulation and navigation modules
C. Guidance and target parameter preparation modules
D. Controller module
E. SC dynamics and kinematics module
F. Visualization module

V. Design Example

Consider the three-axis attitude control problem of a rigid SC with the following nominal inertia matrix in units of $[Kg.m^2]$:

$$J = \begin{bmatrix} 430 & -2 & 4 \\ -2 & 250 & 3 \\ 4 & 3 & 425 \end{bmatrix} \quad (25)$$

The Two Line Element (TLE) which is used to describe the position of a SC:

1 39687U 14021A 15104.17571456 .00000246 (26)
00000-0 10000-3 0 9994
2 39687 051.6201 336.2611 0000555 110.4498
249.6507 14.5383753752965

Actuator dynamics in each axis is assumed as:

$$\frac{u_i}{u_{ic}} = \frac{(50)^2}{s^2 + 2(0.7)(50)s + (50)^2} \quad (27)$$

where u_i is the actual control torque acting along the ith control axis of the SC and u_{ic} is the control torque command with maximum torque saturation limits in each channel $U = (1,0.5,1)[\mathrm{N.m}]$. Taking the damping ratio $\zeta \approx 0.9$ and the natural frequency $\omega_n \approx 0.45\ [rad/s]$ yield to the positive scalars $k \approx 0.4\ [s^{-2}]$ and $d \approx 0.8[s^{-1}]$. The maximum angular rate $|\omega_i|_{max}$ is assumed to be 85% of the high accuracy range $(2\ [deg/s])$ of measuring angular velocity using star trackers. The maximum control acceleration in the maneuvers direction a_{maxp} is chosen to be 60% of U/J_{ii} to accommodate the actuator dynamics, the nonlinear nature of quaternion-based phase-plane dynamics, and control acceleration uncertainty.

A. Model Verification and Controllers Analysis

A simulation study of the described time-optimal nonlinear three-axis quaternion feedback control logic was performed for many closely placed ground targets mission for single imaging and stereo imaging. The mission consists of a sequence of three maneuvers to achieve the following Euler angles sets; [20; -4; -18], [-25; -3; -2] and [25; -3; -1] [deg], as shown in Fig. 10. Figs. 11 and 12 illustrate the control torque generated using the proposed control logic with actuator saturation limit. Fig. 13 shows the SC angular rates for the proposed control logic. In addition, it shows that the SC angular rates during the three maneuvers did not reach to saturation speed of the sensor. Fig. 14 illustrates the SC Euler angles for the proposed control.

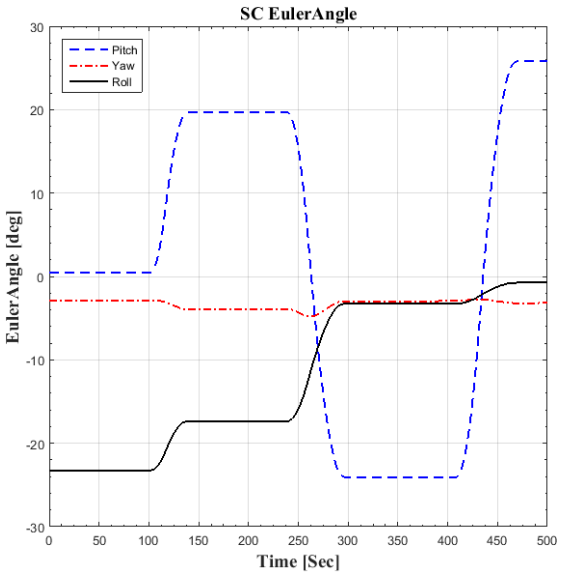

Fig. 10 SC Euler angles time responses for sequence of three maneuvers

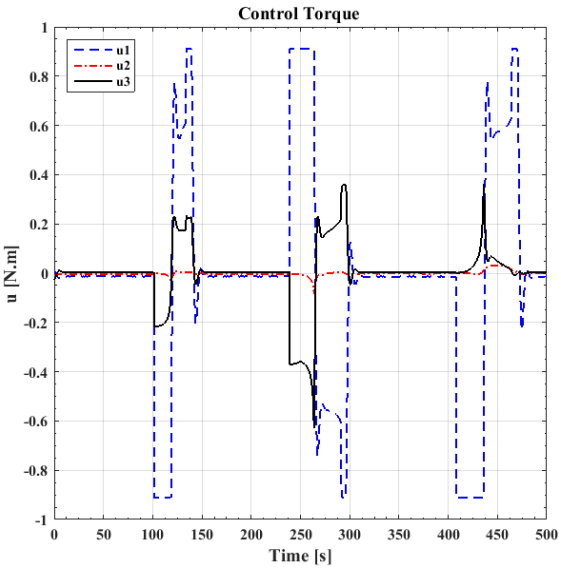

Fig. 11 Control torque using the simulated control logic

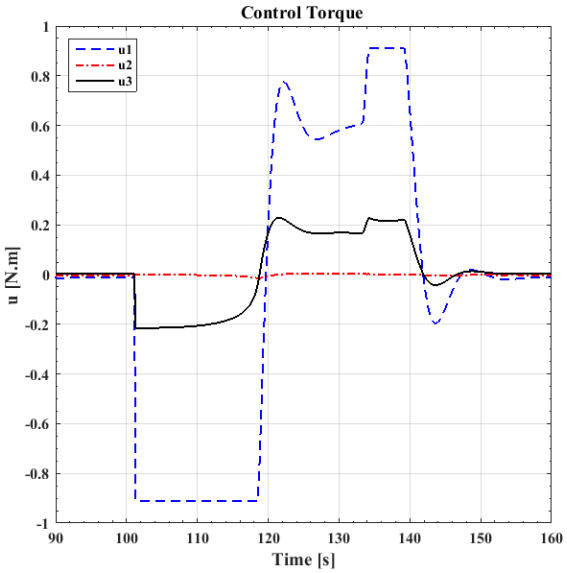

Fig. 12 Control torque using the simulated control logic with actuator saturation limit

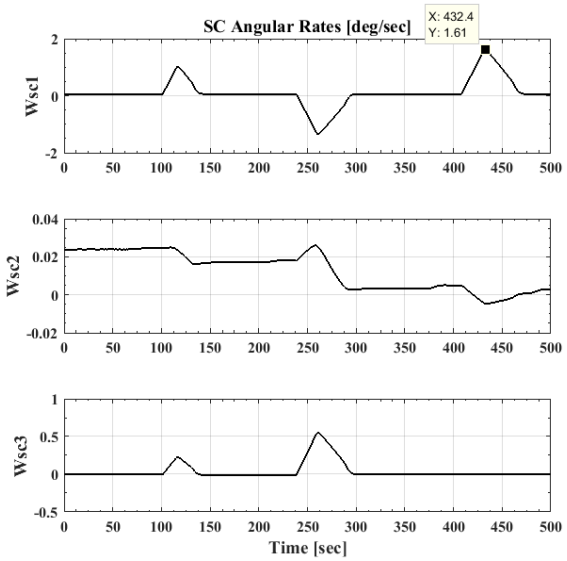

Fig. 13 SC angular rates for the simulated control logic

B. Orbit Simulation Analysis

Fig. 15 shows the SC position vector predicted using SGP4 and verified by the position vector obtained from the Satellite Tool Kit (STK) application.

Fig. 16 shows the SC position vector error (difference between the predicted position vector using orbit propagation via integration of the equation of motion and the extracted position vector from verification data) during time interval 757[s]. Table II illustrates the maximums and the mean values of errors in X-axis, Y-axis and Z-axis.

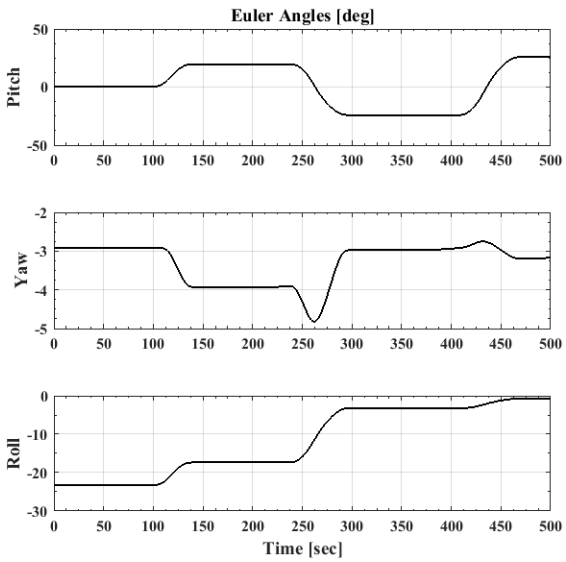

Fig. 14 SC Euler angles for the simulated control logic

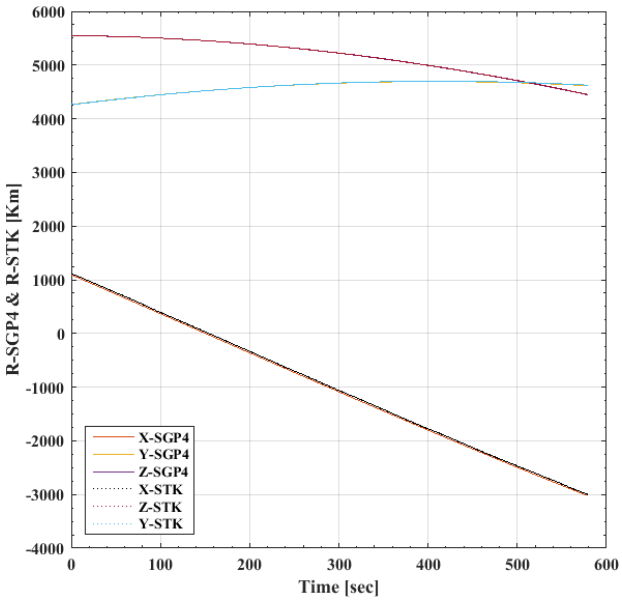

Fig. 15 Position vectors R_SGP4 and R_STK

TABLE II
MAXIMUM AND MEAN VALUES OF POSITION VECTOR ERROR

Error	$\|Error\|_{max}$ [Km]	Mean value [Km]
X	7.942	2.607
Y	5.882	2.054
Z	5.68	1.332

Fig. 17 illustrates the 3D SC trajectory comparison between the results obtained from orbit propagation via integration of the equation of motion using (1) in red color and the verification data in blue color for three orbits. Fig. 18 illustrates the same comparison in 2D for X-axis, Y-axis and Z-axis.

Fig. 19 shows the SC position vector error (difference between the predicted position vector using SGP4 and TLEs

and the extracted position vector from the verification data) during time interval 600 sec. Table III illustrates the maximums and the mean values of errors in X-axis, Y-axis and Z-axis.

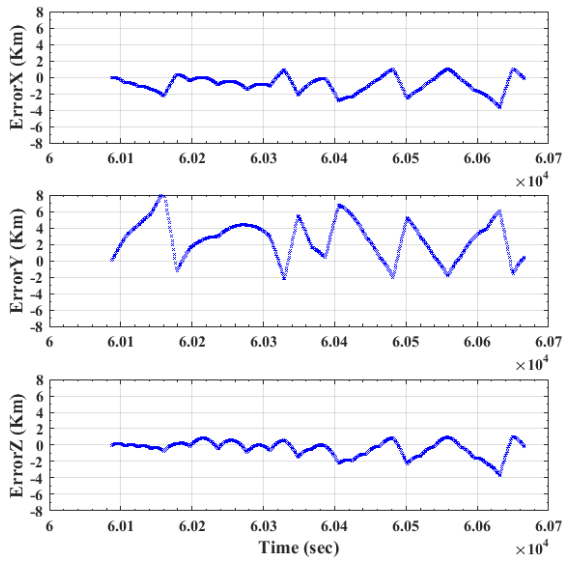

Fig. 16 Error in orbit prediction using orbit propagation via integration of the equation of motion

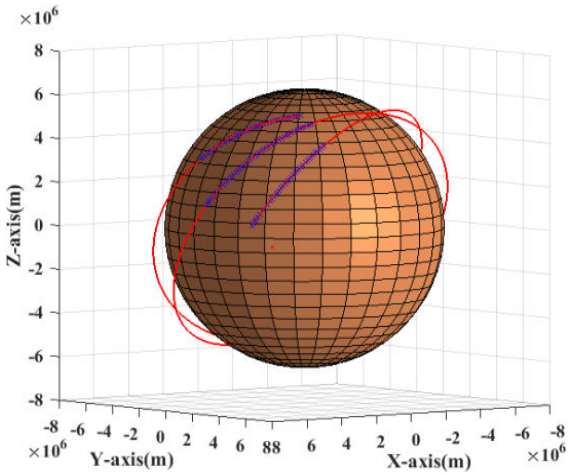

Fig. 17 3D Comparison between the orbit propagation via integration of the equation of motion and the verification data

TABLE III
MAXIMUM AND MEAN VALUES OF POSITION VECTOR ERROR

Error	$\|Error\|_{max}$ [Km]	Mean value [Km]
X	6.174	1.973
Y	3.32	1.107
Z	5.107	0.8877

Fig. 20 illustrates the 3D SC trajectory comparison between the results obtained using SGP4 and TLEs in red color and the verification data in blue color for three orbits. Fig. 21 illustrates the same comparison in 2D for X-axis, Y-axis and Z-axis.

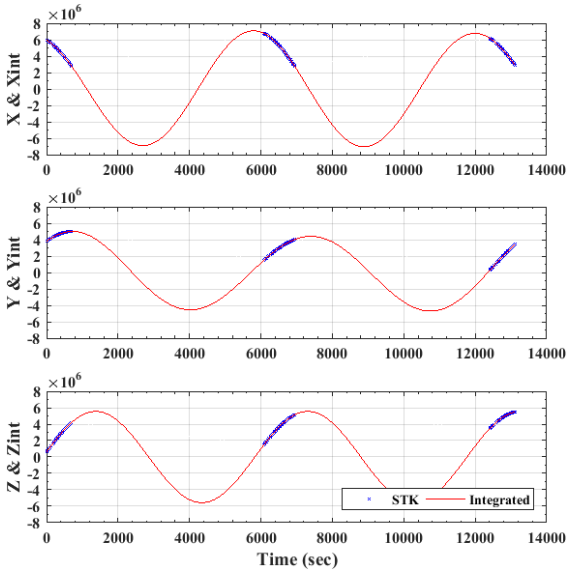

Fig. 18 2D Comparison between the orbit propagation via integration of the equation of motion and the verification data

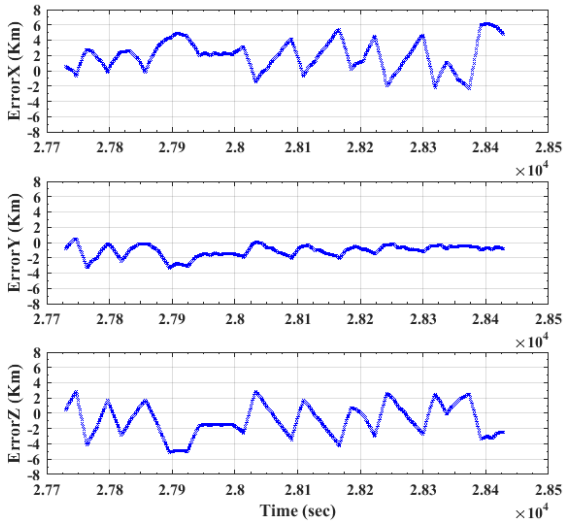

Fig. 19 Error in orbit propagation using SGP4 and TLEs

VI. VISUALIZATION

This simulation provides options for visualizing SC dynamics in a 3D environment; trajectory and attitude, including an interface to V-Realm Builder and VR Sink of Simulink/MATLAB. The visualization of a SC trajectory and attitude appear in Fig. 22. Fig. 23 shows zooming in SC attitude visualization. Fig. 24 illustrates the monitoring process to SC energy ellipsoid.

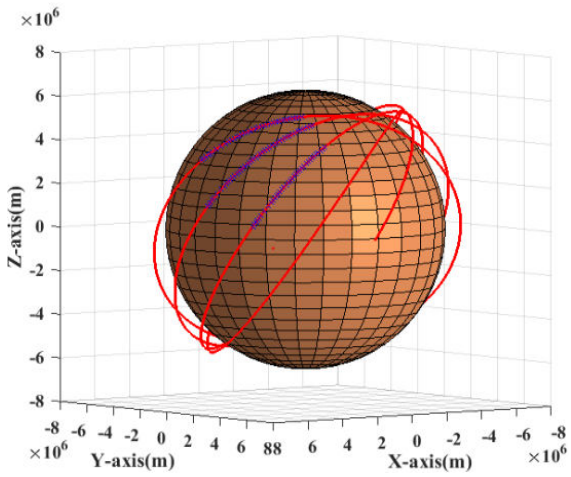

Fig. 20 3D Comparison between the orbit propagation using SGP4 and TLEs and the verification data

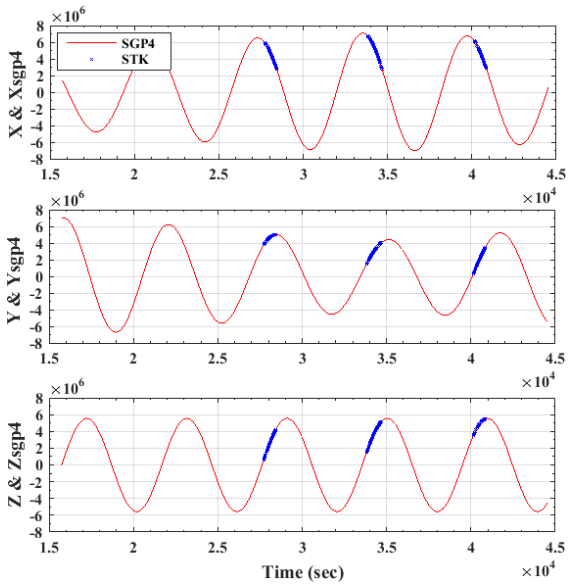

Fig. 21 2D Comparison between the orbit propagation using SGP4 and TLEs and the verification data

VII. Conclusion

Acceptable results for the proposed time-optimal nonlinear feedback control technique are achieved. The results of the orbit simulation achieved the accepted accuracy for the purpose of the formulation of coupled SC orbital and attitude equations of motion. This coupling becomes valuable when actuators do not work, e.g. during communication loss with the SC. The same case gives important orbit estimation using SGP4 and TLEs because it is dependent on the physical observation to the SC. It can give an indication of whether the SC is still in its trajectory and how much it may drift from its normal path.

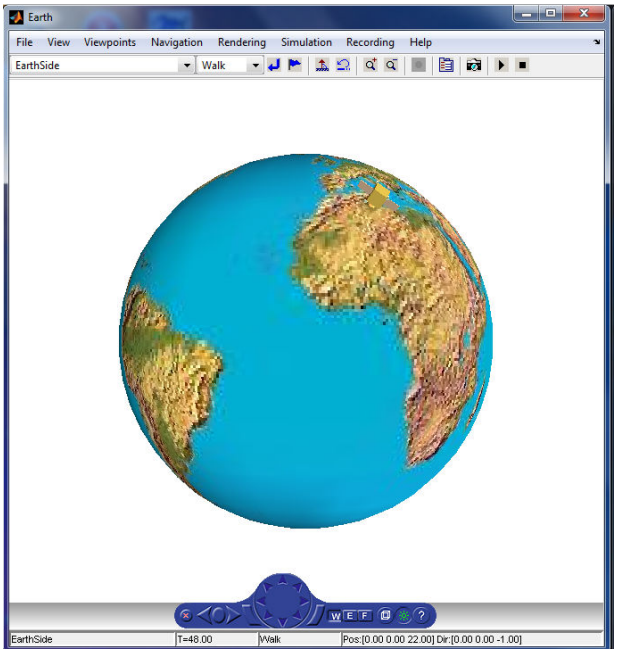

Fig. 22 VR Sink and V. Realm Builder

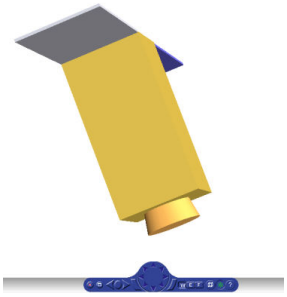

Fig. 23 Visualization of SC orientation

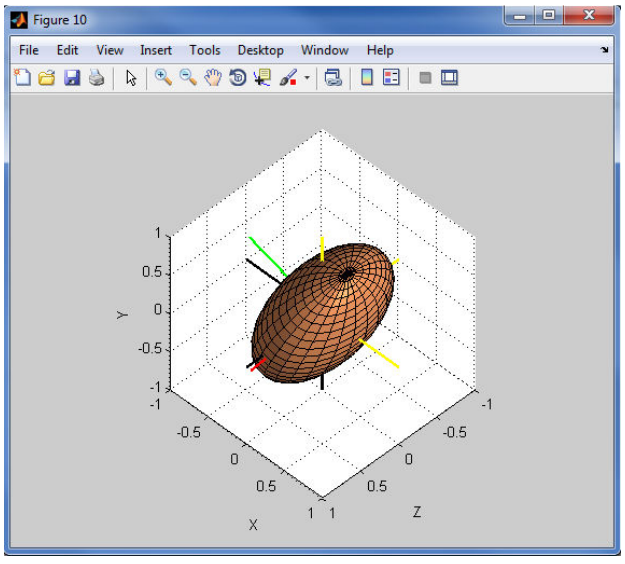

Fig. 24 Visualization of SC energy ellipsoid

REFERENCES

[1] Montenbruck, O., Gill, E., *Satellite Orbits*.: Springer, 2003.
[2] Patrick Daum, "*A Satellite Footprint Visualisation Tool*," Lancaster (U.K.), M.Sc. 2005.
[3] Ashish Tewari, "*Atmospheric and Space Flight Dynamics*," Indian Institute of Technology Department of Aerospace Engineering, Kanpur-India Birkhauser Boston, 2007.
[4] Hoots, F.R., Roehrich, R.L., "*Spacetrack Rep. No.3: Models for Propagation of NORAD Element Set*," Compiled and distributed by TS Kelso, December 1980 (available under: http://www.celestrak.com/NORAD/documentation/spacetrk.pdf stand. Hoots: September 7, 2005.
[5] David A. Vallado, Paul Crawford, Richard Hujsak, T. S. Kelso, "*Revisiting Spacetrack Report #3*," Center for Space Standards and Innovation, Colorado Springs, Colorado, 80920.
[6] Bong Wie, *Space Vehicle Dynamics and Control*. USA: Inc., 1998.
[7] Wertz, J.R., Larson, W.J., *Space mission analysis and design*.: Kluwer academic publishers, 1999.
[8] Syed Zohaib Ali, "*Simulations of a Satellite System for Co-Location in Space*," Department of Earth and Space Sciences - Chalmers University of Technology, Göteborg, Sweden, M.Sc. 2013.
[9] F. Landis Markley, John L. Crassidis, *Fundamentals of Spacecraft Attitude Determination and Control*. New York: Microcosm Press and Springer, 2014.
[10] Marcel J. Sidi, *Spacecraft Dynamics and Control A Practical Engineering Approach*: Cambridge University Press, 1997.
[11] Klaus Wittmann and Willi Hallmann Wilfried Ley, Ed., *Handbook of Space Technology*.: John Wiley & Sons, Ltd., 2009.
[12] Anton H.J. de Ruiter, Christopher J. Damaren, James R. Forbes, *Spacecraft Dynamics and Control An Introduction*. United Kingdom: John Wiley & Sons, Ltd, 2013.
[13] Zhang Xuxi, Liu Xianping, "*Chattering Free Adaptive Sliding Mode Control for Attitude Tracking of Spacecraft with External Disturbance*," in 33rd Chinese Control Conference, Nanjing, China, July 28-30, 2014, pp. 2224-2228.
[14] Junkins, J. L. and Turner, J. D., *Optimal Spacecraft Rotational Maneuvers*. Amsterdam, Netherlands: Elsevier Science Publishers, 1986.
[15] Wie B, Bailey D, Heiberg C, "*Rapid multitarget acquisition and pointing control of agile spacecraft*," Journal of Guidance, Control, and Dynamics, vol. 25, no. 1, pp. 96-104, January–February 2002.